https://doi.org/10.48047/AFJBS.8.10.2026.22-50

African Journal of Biological Sciences

Journal homepage: http://www.afjbs.com

Research Paper Open Access

Instrumentation Design and Fabrication for Detecting Micro–Voltage Potentials in Spinach Plant

Ndung'u Ruth Wairimu[1], Kamweru Paul Kuria[2]*

[1] Basic Sciences, Tharaka University College. E-mail:ruthwairimu237@gmail.com
[2] Physical Sciences Department, Chuka University. E-mail: pkkamweru@chuka.ac.ke
*Corresponding Author

Volume 8, Issue 10, Oct 2026

Received: 20 July 2026

Accepted: 15 Sep 2026

Published: 27 Oct 2026

doi:10.48047/AFJBS.8.10.2026.22-50

Abstract

Electrical signals in plants are minute and surrounded by a lot of electrical noise. There was need therefore to design an instrumentation that detects, amplifies and filters the signal from the noise. This chapter reports on the design of an innovative instrumentation, starting with circuit design and implementation of the general purpose of the op-amp. The analysis of the op-amp schematic by simulation was done using LT spice software. Simulation results enabled the extraction of useful characteristics of the signal i.e. the frequency and the magnitude. The electrical signal obtained from the plants, was about 25 mV in magnitude and 1Hz in frequency. The signal was subsequently amplified to 200 mV and filtered for further analysis. This was made possible by incorporating a digital lock-in amplifier, connected to the developed amplifier kit (with the opamp). The extra-cellular recordings were performed by inserting Ag/AgCl microelectrodes, fabricated by this study, into the stem and leaf petiole parts of the spinach plant. The use of the lock-in amplifier made this work unique and also improved on sensitivity and noise filtration of the potential signal of the spinach plant.

Key Words; Electrical signals, Spinach plant,

Simulation, Lock-in amplifier

1. Introduction

Electrophysiological signal in plant is a weak electrical signal, which can fluctuate with change of environment (Cai & Qi, 2017). Different methods have been used to measure electric potentials. Extracellular recording (Xu *et al.,* 2021, Zhao *et al.,* 2013, Stolarz *et al.,* 2021), Intracellular recording (Zebelo *et al.,* 2015) and patch-clamping (Samhita *et al.,* 2021; Isayenkov *et al.,* 2010) have widely used to measure electrical signals. Dong-Jie *et al.,* 2013 used the VSD $DiBAC_4$ which has a low toxicity and a slower response time (in hundreds of milliseconds) compared with fast response VSDs. The method was used to record both APs and VPs in *H. annus* (Zhao *et al.,* 2014).

To measure ES in plants, amplification is a necessity due to the minute nature of the signals. For example, Cai & Qi (2017), designed an amplification detection system for plant electrical signal acquisition by using integrated Op-amps (CA 3140, AD620 and INA118, patch electrode, data acquisition card (NI USB-6008), computer and shield box. The graphite patch electrode was used to measure the electrical signals on the surface of the plant. The amplification detection system can make nondestructive acquisition for *Acquatic Scindapsus* and *Guaiben* with high precision, high sensitivity, low power consumption, high common rejection ratio and working frequency bandwidth. Stress experiments were conducted through the system. Their results showed that electrical signals were produced in the leaf of *Acquatic Scindapsus* under water-logging stress and under pressure. The amplification should however be coupled with filtration to improve the signal to noise ratio.

The next challenge in detection of ES in plants is the electrodes to use. In one study, ES in plants were detected using a cotton thread soaked in an experiment solution (KCl 0.1mM, $MgCl_2$ 0.1mM, $CaCl_2$0.5mM, $Na_2SO_4$0.05mM) (Wang *et al,* 2009,). One end of the cotton thread was covered with a soft plastic tube which contacted the system surface of the plant, while the other end was soaked in a 25ml volume chamber of the electrode supported with an adjustable holder, and the electrode was inserted into a chamber containing the experiment solution, where the solution was renewed every other day. The signal from the electrode was transmitted into a CA3140 impedance converter, which is an integrated circuit operational amplifier that provides very high input impedance, very low input

current, and high speed performance and is then connected to an AD620 amplifier. After amplification, the amplitude range of the electrical signals was ±4000 mV. Several studies applies the use of the Ag/AgCl electrodes e.g. (Gurovich & Hermosilla, 2009; Oyarce & Gurovich, 2011; Gil *et al.,* 2009). The Ag/AgCl electrode has the advantage that it is nonpolarizable and therefore its potential is not affected by current flowing through it.

The extracellular recording, intracellular recording and patch recording methods can only detect the extracellular potentials of the cells around the electrode (using metal electrodes) or measure the transmembrane potential change of single cells (using microelectrodes (Dong-Jie *et al.,* 2013). There are limitations in both extracellular and intracellular recordings in terms of being able to distinguish changes in the electrical potential from multiple cells or different tissues in the stem of a plant. Other methods, for example, optical recording may overcome these limitations using voltage-sensitive dyes (VSDs) and allow monitoring of the bioelectrical activity at multiple sites with high resolution. This method has a high spatial resolution that makes it possible simultaneously measure the distribution of the electrical activity from different tissues in *vivo in situ* in a plant (Dong-Jie *et al.,* 2013)

This study therefore sought to fabricate a portable kit, with Ag/AgCl electrodes and a lockin amplifier that will innovatively measure small EP in spinach which is leafier and whose height above the ground is much lower and grown more in green houses when compared to other woody plants like avocado.

2. Materials and Method

2.1. Circuit Materials and Kit Design

The materials used were; specifically designed electrodes (section 6.1), lock-in amplifier (section 2.3), voltage amplifier circuit (section 2.2) and a computer to visualize the spinach plant EP signal. These were connected as will be shown in section 3.6.3. The voltage amplifier circuit was simulated using LT SPICE software as shown in section 3.4.

2.2. Voltage Amplifier Circuit

This study designed an electrical circuit, with a suitable op-amp, capable of amplifying weak (low voltage) plant signal as shown in *Figure **1***.

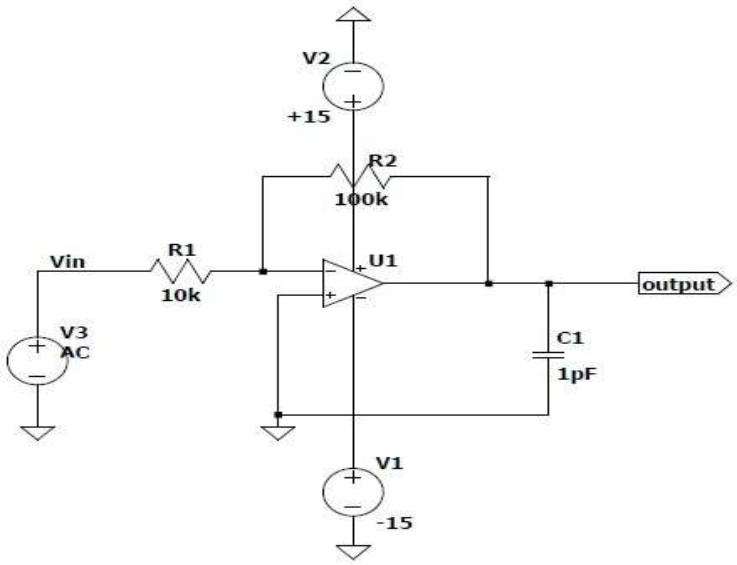


Figure 1: Schematic diagram of electrical signals amplifying circuit for plant

To actualize the above circuit, an op-amp LF356N voltage amplifier was used. This amplifier is excellent for low noise applications using either high or low source impedance. It features low input bias and (Ren *et al.,* 2019) offset currents/low offset voltage and offset voltage drift or common-mode rejection. The circuit was designed for internal compensation and large differential input voltage capability. Other components that include a capacitor (1 μF) and two resistors (10 KΩ) and (100 KΩ) that were fixed to the breadboard and connected as follows; first, the resistors were connected to pin 3 and 6 of the amplifier, secondly, the capacitor was also connected to pin 3 and 6 just the same as the resistor, a jumper wire was used to interconnect the components of the circuit without soldering.

2.3. Lock-in Amplifier

In this study, very minute signals (magnitude at the micro scale) against a background of high noise were anticipated. To improve signal to noise ratio, the amplified voltage signal from the plant is fed to the digital lock- in amplifier, before viewing and processing in the computer or digital oscilloscope. The lock-in amplifier helps to detect very small signals that would otherwise get lost in the noise of even the best amplifiers.

The lock-in amplifier has a circuit as shown in Figure 2, and consists of three main parts: the input amplifier, a synchronous demodulator and final low- pass filter/ amplifier that finally outputs the DC signal (Bhagyajyoti *et al.,* 2012).

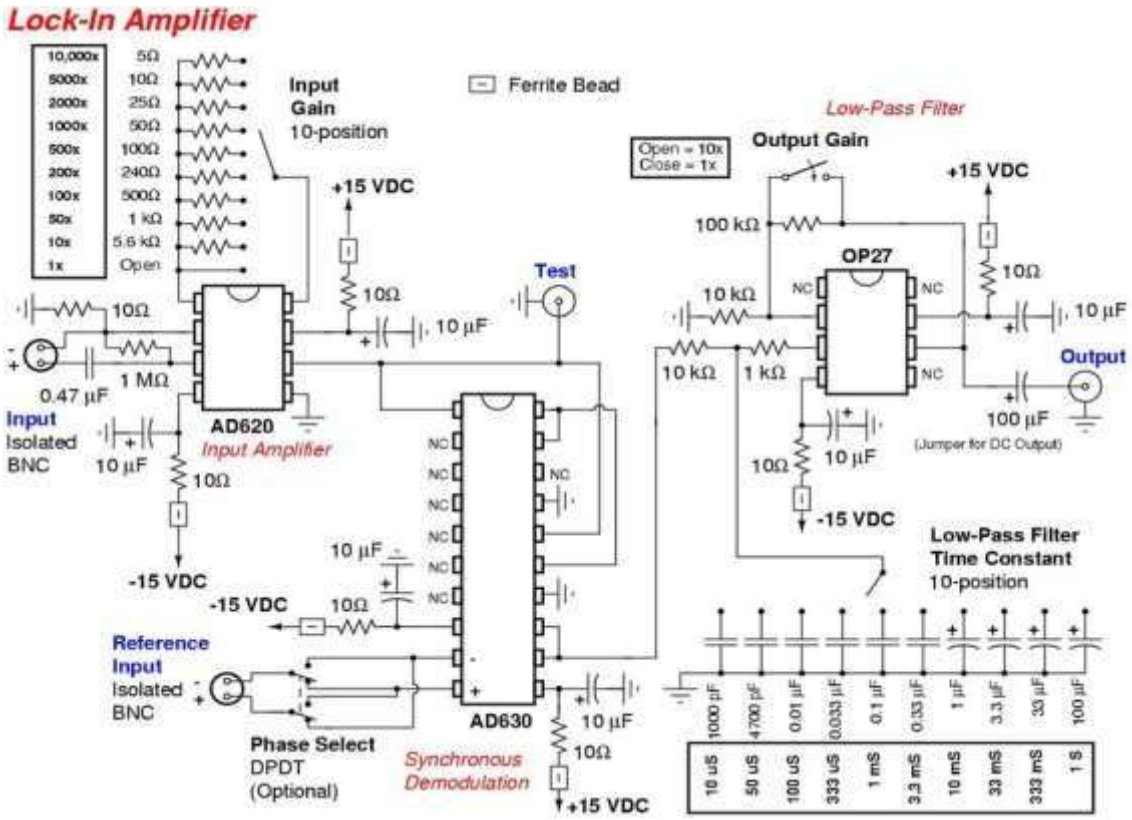


Figure 2: Lock-in amplifier circuit Obtained from, Sengupta *et al.,* (2005).

The input amplifier (AD620) amplifies the input signal using a variable gain resistor. The amplifier does not just amplify the desired signal, but the input signal as a whole i.e. noise is also amplified. The synchronous demodulator (AD630) is essential ingredient in the lock-in amplifier and is what does the actual signal mixing. This is where the reference signal is inputted. The low-pass amplifier (OP27G) filters noise in the modulator signal and outputs our desired DC signal that determines the strength of the lock-in. The lock-in amplifier is used to detect a modulated signal that is typically buried in a large noise background. To do so, a reference signal is supplied into the lock-in. This reference provides both the frequency and phase of the expected output. To narrow its output to a small bandwidth around the expected frequency at the expected frequency at the specified phase, the signals are multiplied together. Random noise and the reference are uncorrelated and their multiplied values fluctuate in time and average to zero. A low pass filter picks out

the part of the signal that is correlated with the reference essentially by averaging the output of the mixer; this is the lock-in output.

3. Circuit Simulation

The aim of this simulation was to verify and characterize the performance of the op-amp and the circuit in *Figure **1***. Simulation was done using LT SPICE software, a free circuit simulator available from the internet. To simulate a schematic space was created and opamp selected from the component library. The positive, negative and output terminals of the op-amp connected to the rest of the circuit as in *Figure **1*** in section 3.3.

3.1. Simulation by powering both positive and negative rails

Both positive and negative rails of an op-amp were powered because the op-amp is only able to output a value between the ranges of voltages it is powered with. The positive rail of the op-amp was powered with 15 V DC supply source and then the negative rail of the op-amp is connected to ground as shown in *Figure 3*.

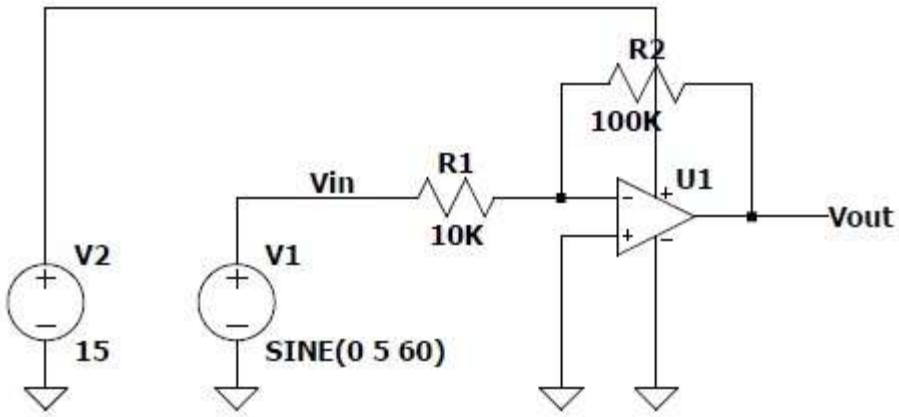


Figure 3: A schematic circuit with only positive rail powered

It is expected that the output signal is inverted and amplified to five times the size of the input signal. The transient analysis command was set and the simulation run. The device limitation was changed by powering both rails of the op-amp with -15 V source as shown in *Figure **4***. This allowed the output signal to vary between +15 V and -15 V. Another voltage source with the positive terminal was connected to the negative rail of the op-amp, the negative terminal to the ground and a value of -15 V as shown in the *Figure **4***.

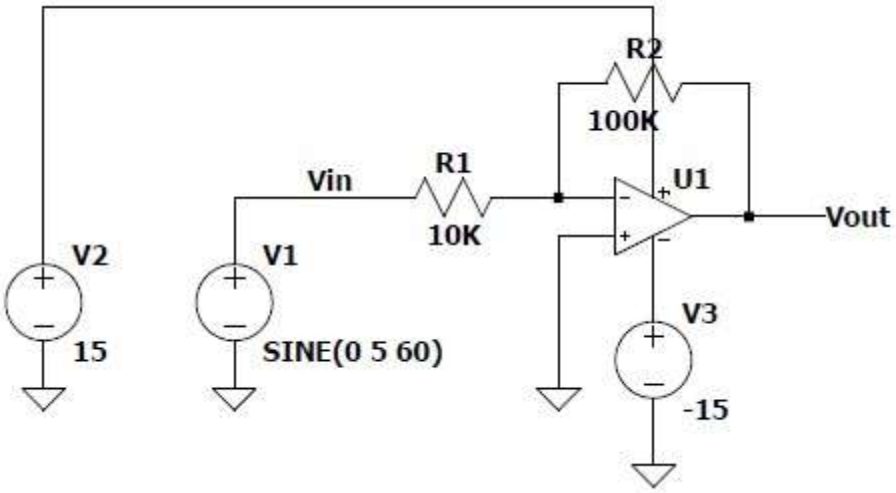


Figure 4: A schematic circuit with both rails powered

The circuit was re-simulated. The results are as shown in Figure 5 and Figure 6 for the positive rail and negative rails powered respectively.

The simulation (Figure 5) shows that the input voltage varies between -5 V and 5 V as expected. The output voltage is inverted and amplified to five times the size of the input waveform, but half of the time.

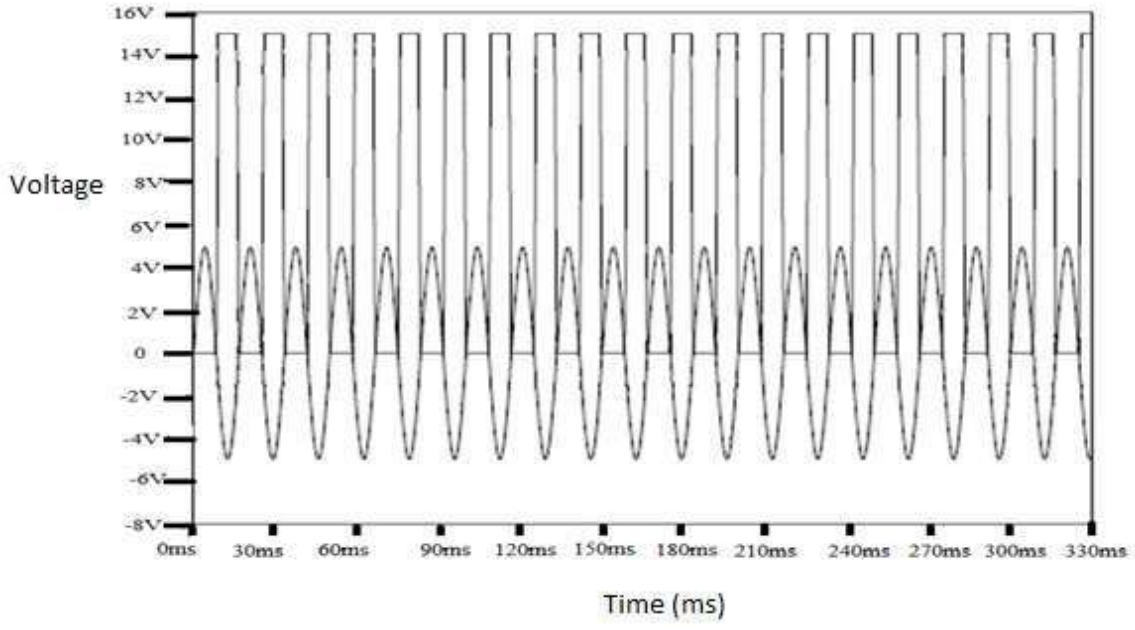


Figure 5: Simulation result with only positive rail an op-amp powered

Now the output is the desired waveform (in Figure 6), inverted and five times larger than the input waveform.

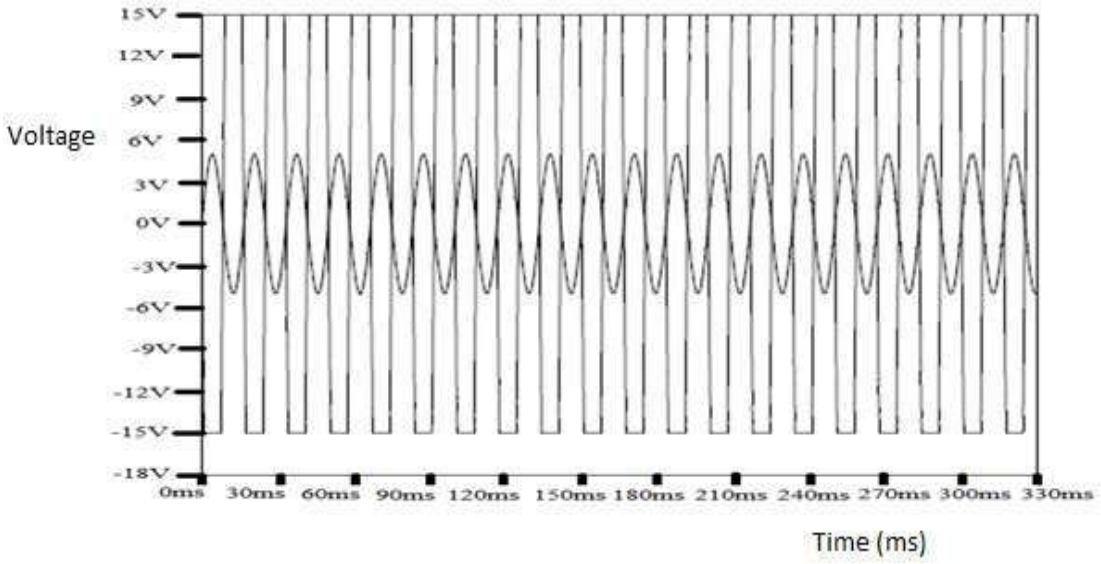


Figure 6: Simulation result with both rails of an op-amp powered.

3.2. Frequency response to op-amp

The circuit in
Figure *7* was drawn on the schematic space. The AC analysis command was set with the input selected as a type of sweep decade, number of points 100, start frequency 100 Hz and stop frequency as 40 MHz, two resistors were used; 10 KΩ and 100 KΩ. Higher resistances were used because they are considered to be less noisy.

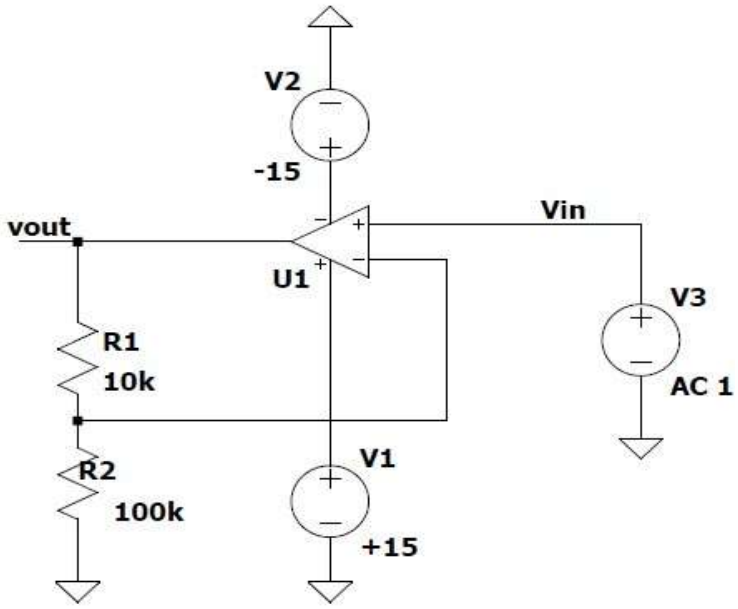


Figure 7: A schematic circuit to show frequency response to op-amp

For a practical op-amp, the phase shift is dependent on the frequency of the input signal. At high frequencies, the phase difference approaches zero and a portion of the output signal is fed back to the input in phase with the input. This changes the feedback mechanism from negative to positive and the amplifier may become unstable or marginally stable. The Gain begins to decrease at such a low frequency as shown in figure 14.

The simulation result in Figure 14 shows that, at very low frequency, the op-amp amplifies the maximum open-loop.

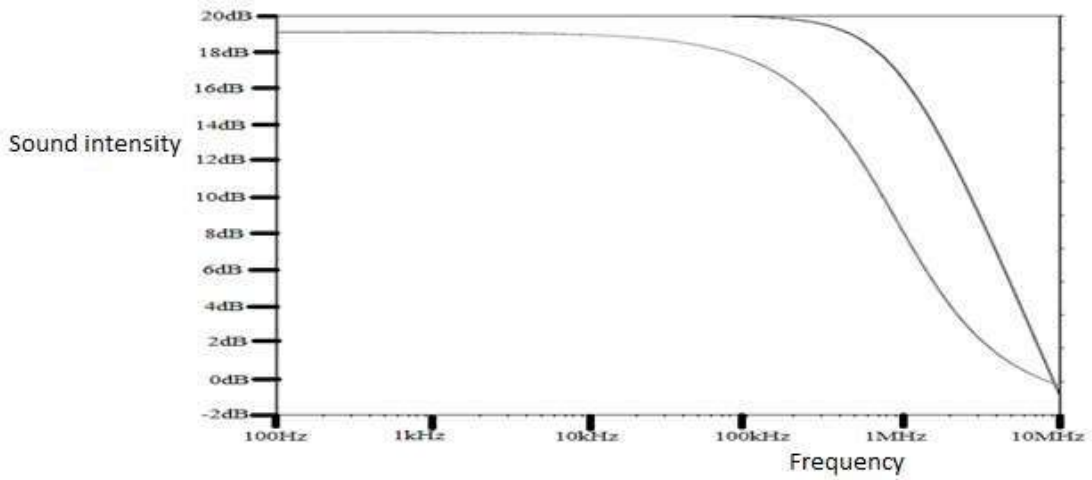


Figure 8: Simulation result for frequency response to op-amp

As frequency increases, gain decreases, with the prominent transition from stable gain to decreasing gain occurring at the corner frequency which in this case is 10 KHz Eventually the slope stabilizes, and the gain decreases by 2 dB for every factor of 10 increases in input frequency. The frequency at which the op-amp's gain reaches 0 dB is called unity-gain and in this case is 10 MHz denoted by f_t. This value indicates the frequency at which the opamp stops functioning as an amplifier, and it also gives a convenient way to calculate the op-amp's open loop gain at a given frequency.

3.3. Noise Analysis and Simulation

Noise analysis involves keeping track of individual noise sources and how these sources add together to produce a total output noise. This study did noise simulation using the circuit in Figure 9, with a resistive voltage divider.

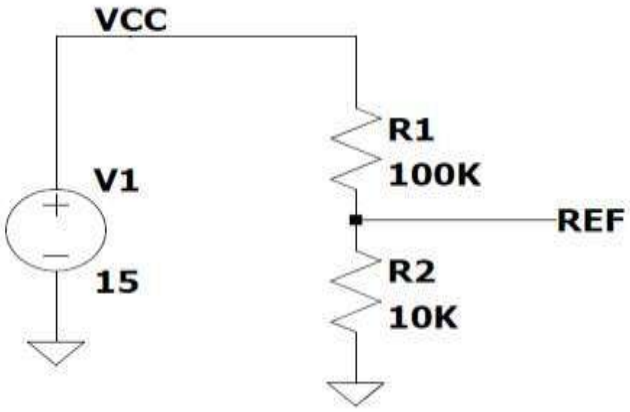


Figure 9: Schematic diagram for noise analysis by applying a resistive voltage divider

This is used to establish a voltage reference or bias in a circuit with a single supply voltage. Resistors produce "thermal" noise, and the amount of noise depends on the value of the resistance, the bandwidth and the temperature. The output was taken as the point in the circuit where all individual noise sources combines into a single value. In this case 'REF' was used. For the input power supply V_1 was used and it is a noise-free source. For the type of sweep, decade was used and the number of points per decade, 100 was used. Start and stop frequencies specify the frequency range of the analysis and here, 1 and 100 K was used then the simulation is run.

With a resistive voltage divider, the simulation is as shown in Figure 10. The plot shows a flat line at 12.277 $nV/Hz^{1/2}$ (The figures were obtained from scaled graph using the LT Spice software). This is the total of individual noise sources added together to produce the noise at the input.

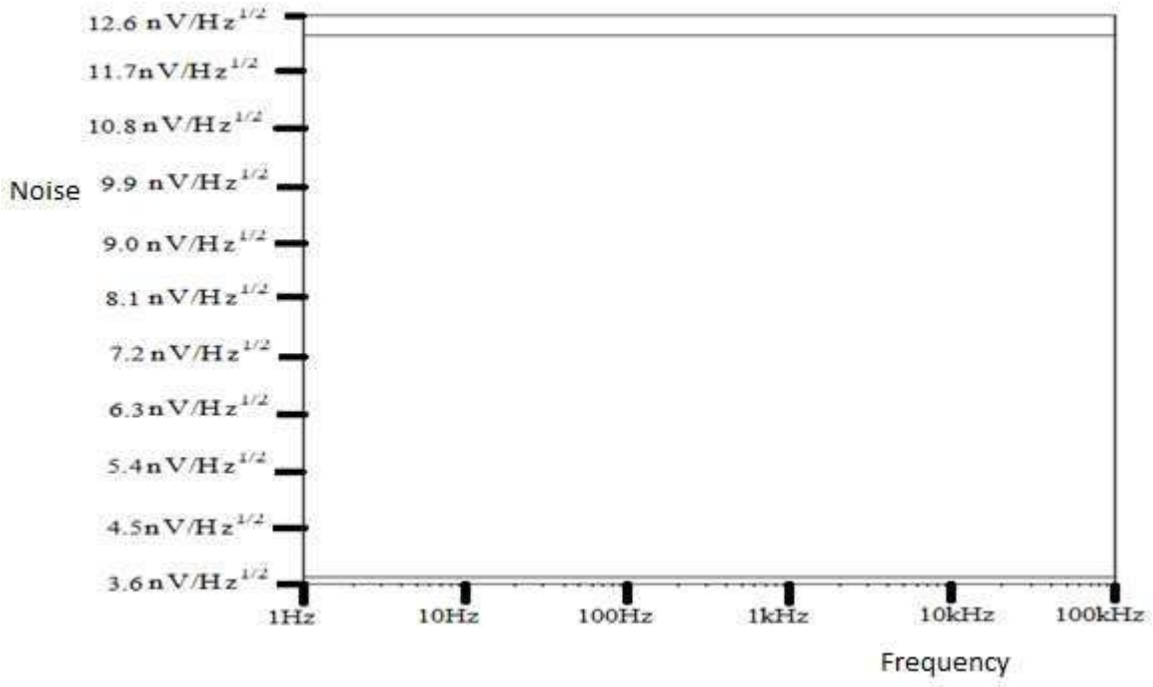


Figure 10: A simulation with a resistive voltage divider

The study experimented the addition of a filter. The set up remained as in Figure 9, but a capacitor is added to filter noise from the power supply as shown in Figure 11.

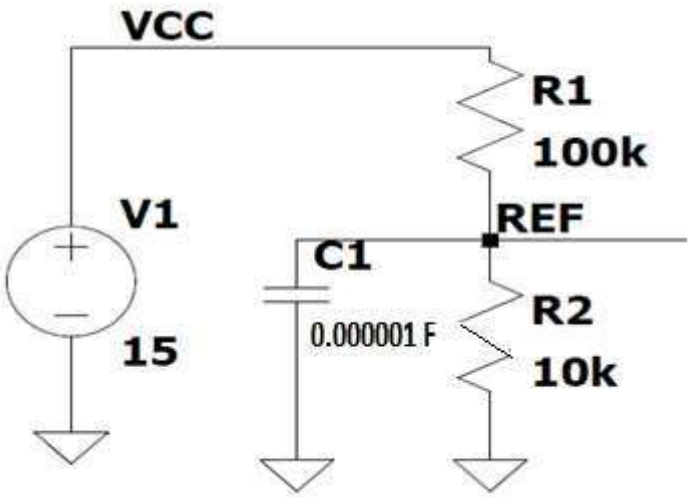


Figure 11: Schematic diagram for noise analysis by adding a filter

The capacitor also filters noise from R_1 and R_2. The effects of adding a capacitor filter is simulated and shown in Figure 12.

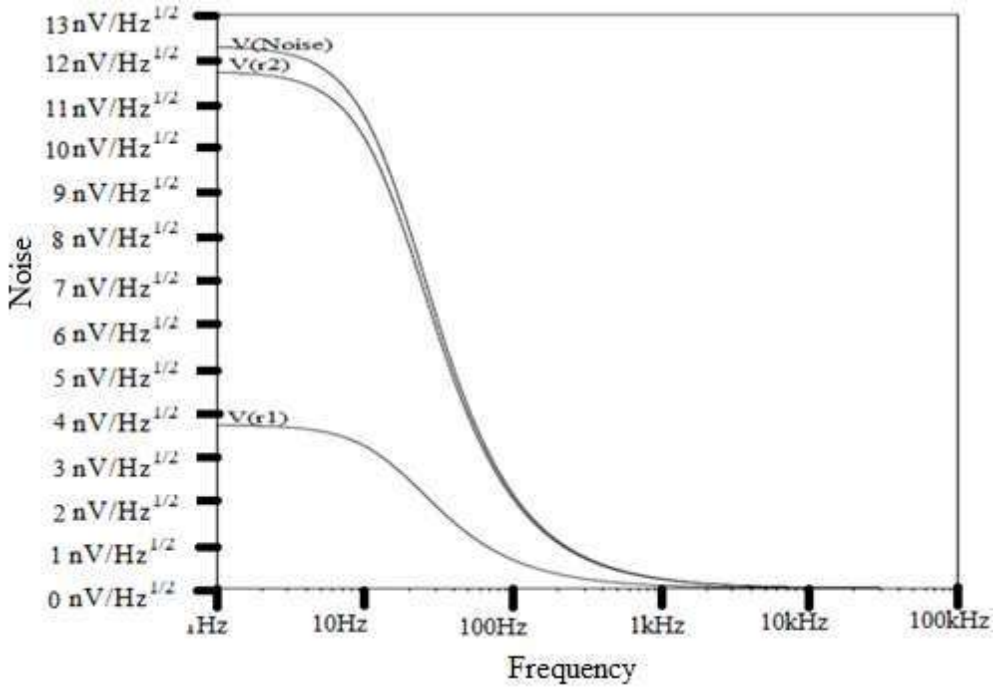


Figure 12: Noise simulation by adding a filter

V (r1) represents the noise from resistor 1 (3.73 $nV/Hz^{1/2}$) and V (r2) represents the noise from resistor 2 (11.8 $nV/Hz^{1/2}$). It is noted that noise at low frequencies has not changed,

but noise is filtered at higher frequencies. The resistor and the capacitor form a low-pass filter.

The third simulation included an amplifier and the set-up is as in Figure 19.With the inclusion of an op-amp, simulation output was changed to 'BREF' and simulation run again. The circuit is shown in Figure 13.

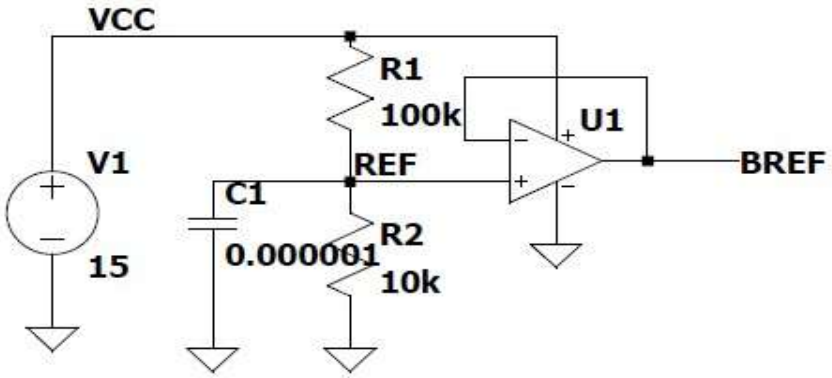


Figure 13: Schematic diagram showing noise analysis by adding an amplifier

When the circuit in *Figure 13* was simulated, the results obtained are as shown in ***Figure 14***.

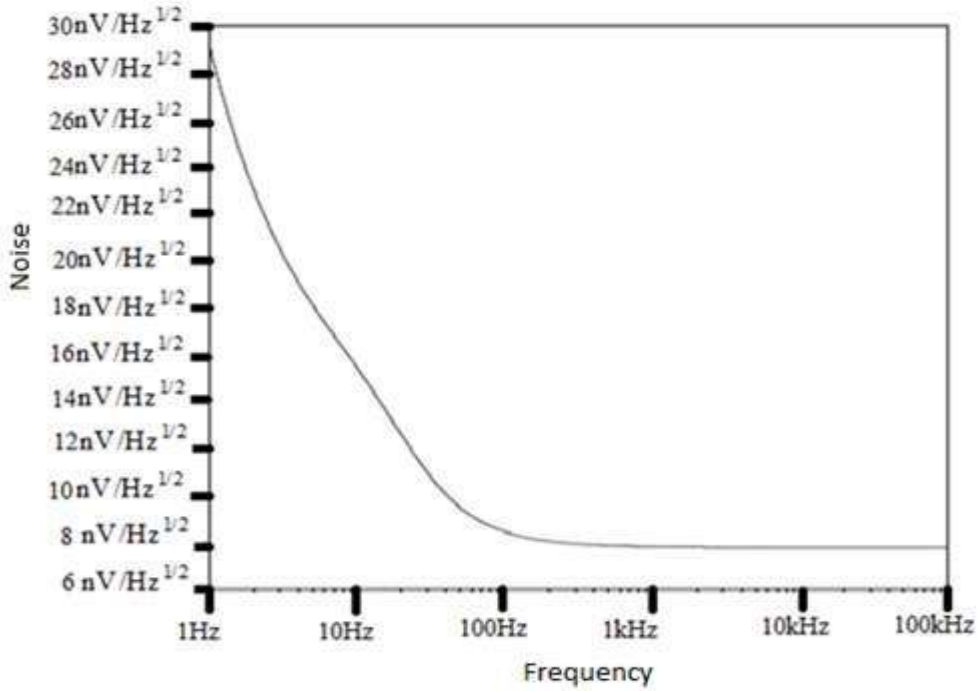


Figure 14: A simulation of noise by adding an amplifier

Noise at lower frequency has now increased from 12.277 nV/Hz$^{1/2}$ to 29.53 nV/Hz$^{1/2}$ (figures drawn obtained from scaled graph on LT Spice software) due to noise from the op-

amp, and higher –frequency noise has returned because the addition noise of the opamp is not filtered out. It is seen that the op-amp noise is greater than the noise from the resistive divider at low frequencies.

Lastly, this study investigated the effect of noise reduction by addition of 'noiseless' resistors. This is by adding the command "noiseless" in LT Spice VIII simulation software to the value of the resistor as shown in Figure ***15*** and the simulation run.

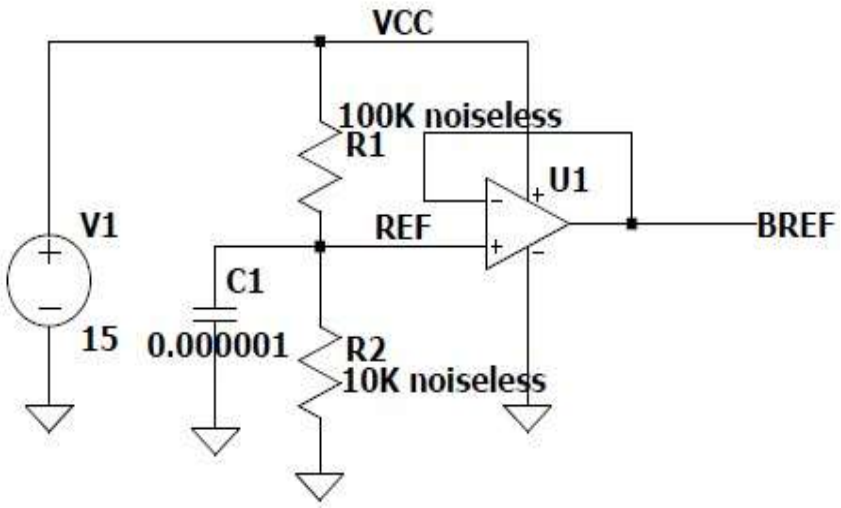


Figure 15: Schematic diagram showing noise analysis by adding noiseless to resistors

Adding noiseless to resistors comands the LT spice to ignore the resistors as noise source. The noise at the lower frequency has now gone down from 29.53 $nV/Hz^{1/2}$ to 26.42 $nV/Hz^{1/2}$ as shown by Figure 16.

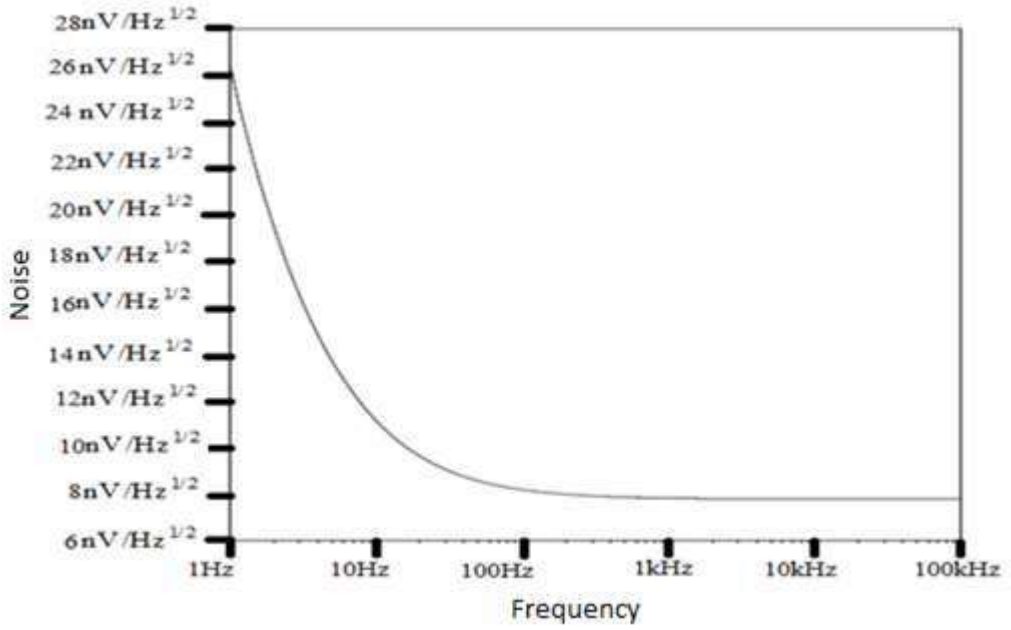


Figure 16: A simulation of noise by adding noiseless to resistors

4. Spinach Electrical Signal Detection and Characterization

Figure 17 shows how the components are interconnected to make a complete instrumentation for electrical measurement in this work and how the signal from the plant is fed to the voltage amplifier, lock-in amplifier the to the computer. Electrical signals on the spinach plant were detected after the plant was exposed to light/dark and water and lack of water conditions.. The specially made silver electrode were pierced at different positions of the spinach plant i.e. the stem and leaf petiole. The circuit was turned on and waited until the numerical digit of voltage stabililized. The voltage data was saved in the computer.

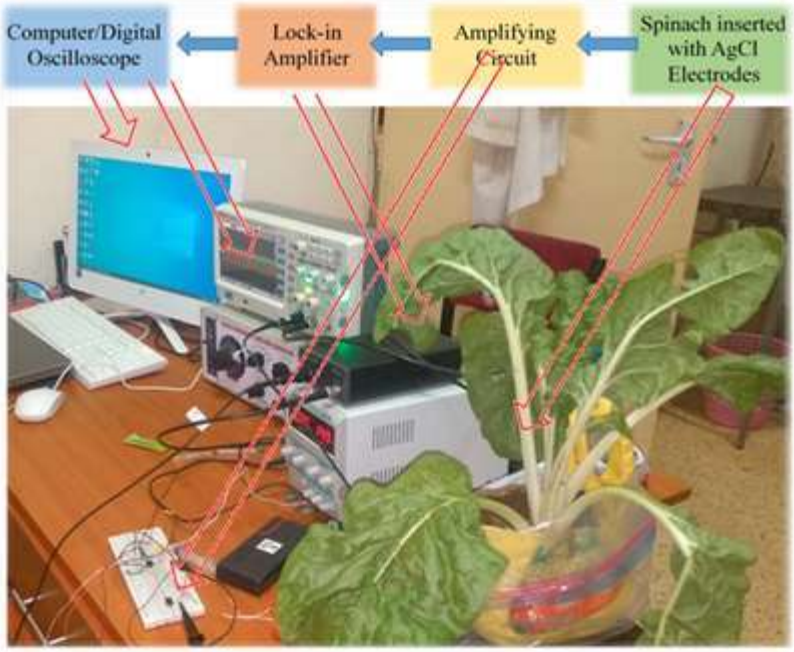


Figure 17: Electric potential measurement instrumentation showing how the signal from the plant is fed to the voltage amplifier, lock-in amplifier then to the computer

The results are as shown by figure 25 and figure 26. Voltage differences between the base of the stem and leaf petiole were measured and recorded. For electrical potential measurement, the surface electrode technique was used. The electrodes were inserted at about 5 cm above the stem and leaf petiole. The electrodes used consisted of a silver wire (99.99% Ag) chlorinated in a solution of HCl and attached of a stainless needle filled with a solution of KCl in which the wire was inserted. Ag/AgCl micro-electrodes were made locally using a silver wire, chlorated in a solution of HCl using a differential voltage to obtain an Ag/AgCl coating. The wire was inserted in a stainless steel hypodermic needle filled with KCl solution; both ends were heat-sealed with polyethylene. The Ag/AgCl electrodes were connected to amplifier to detect the microscale signal from the spinach plant. This voltage was stored on the computer for later analysis. The electrode located on the leaf served as the recording electrode while the electrode located on the stem served as the reference. A schematic diagram of the arrangement of the electrical potential measurement system is shown in Figure 17.

5. Conclusion and Use of the Simulation Results

The simulation results gave insights of the voltage amplifier circuit shown in figure 9. It was possible to match simulation results with an analytically derived conclusion and also show significance of magnitude changes in parameters. It was possible to predict outcomes where otherwise the study could have used trial and error method to select parameter values. The performance of the op-amp LF 356N was verified and characterized using simulation and the results were used to fabricate the voltage amplifier kit shown in figure 26.

6. Results

6.1. Micro-Electrodes

The micro-electrodes were designed and constructed locally following procedures from literature (Ives & Phelan, 2010; Miah *et al.,* 2019; Moore *et al*, 1990; Lito & Camões, 2009). These micro-electrodes consisted of silver wire 0.3 mm diameter and coated with a Silver Chloride (AgCl) film, which was achieved by applying a voltage of 2.5 V in a Hydrogen Chloride (HCl) solution for 30.

$$Ag + Cl^{-} \rightarrow AgCl + electron$$

The wire was then inserted in a hypodermic needle 0.6 mm in diameter filled with a solution of 3.5 M KCl. Both needle ends were sealed with a modelling clay coating.

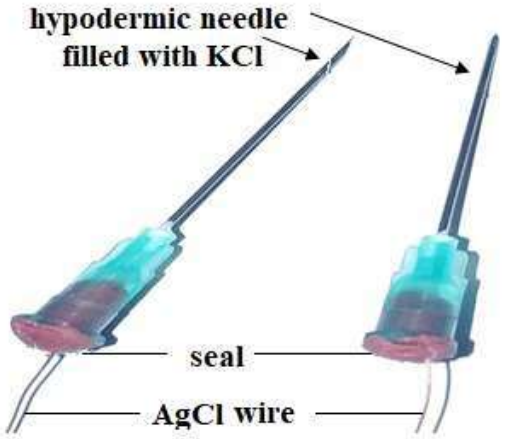


Figure 18: Ag/AgCl electrodes fabricated by this study using a hypodermic needle, KCl, AgCl wire.

6.2. Voltage Amplifier Kit

The plant electrical signal is a weak low-frequency signal and the amplitude ranges from tens of microvolts to the tens of millivolts (Zhao *et al.,* 2013). Such weak signal is generally flooded in strong noise background, which puts forward request for signal extraction and analysis techniques (Jingxia and Weimin, 2011), hence the reason for fabrication of the voltage amplifier kit. Previous studies have shown that the frequency of the plant electrical signal is generally less than 5 Hz (Brenner *et al.,* 2006). An op-amp voltage amplifier was fabricated using an LF 356N op-amp which is an excellent amplifier for low noise applications using either high or low source of impedance. Other components included a capacitor (1 μF) and resistors (10 KHz and 100 KHz) as shown in Figure 19.

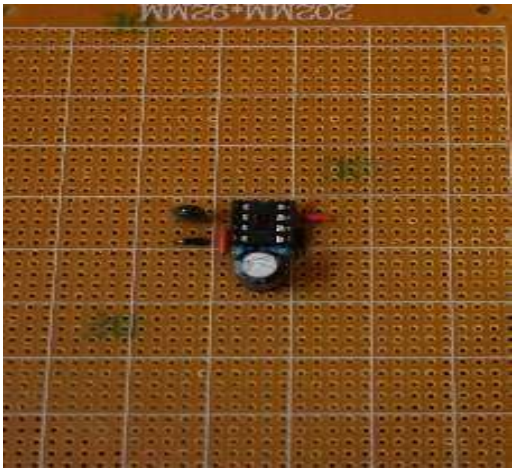


Figure 19: Components of the LF 356N amplifier on a prototype board

The components are interconnected by jumper wires as shown by Figure 20.

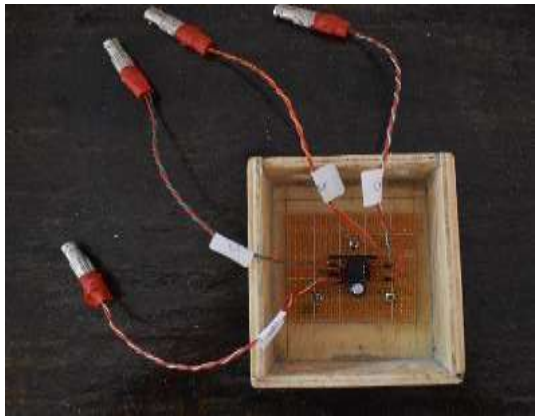


Figure 20: Components interconnected with jumper wires

6.3. Instrumentation Kit Assembly

The BNC connectors were used to connect the amplifier with other components in the circuit as shown in Figure 21 and Figure 22.

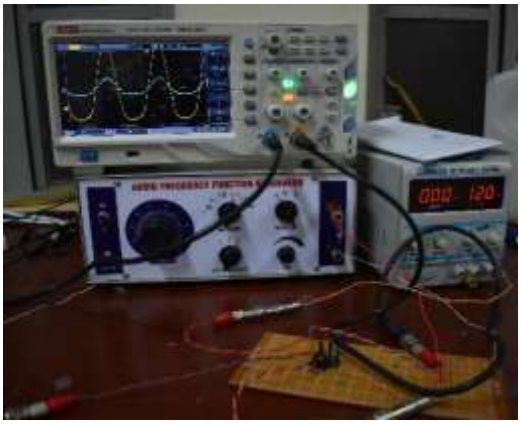


Figure 21: Testing the workability of the amplifier



Figure 22: Voltage amplifier connected to other components of the circuit

6.4. Electrical Signal at the Time-Frequency Domain

The electric signal was analyzed in time-frequency domain. Analysis in time domain treats plant electric waves as a function of time. Time-frequency analysis reflects substantive characteristics of plant signals more deeply and effectively. Test and time domain on spinach plant in normal condition is as shown in Figure 23.

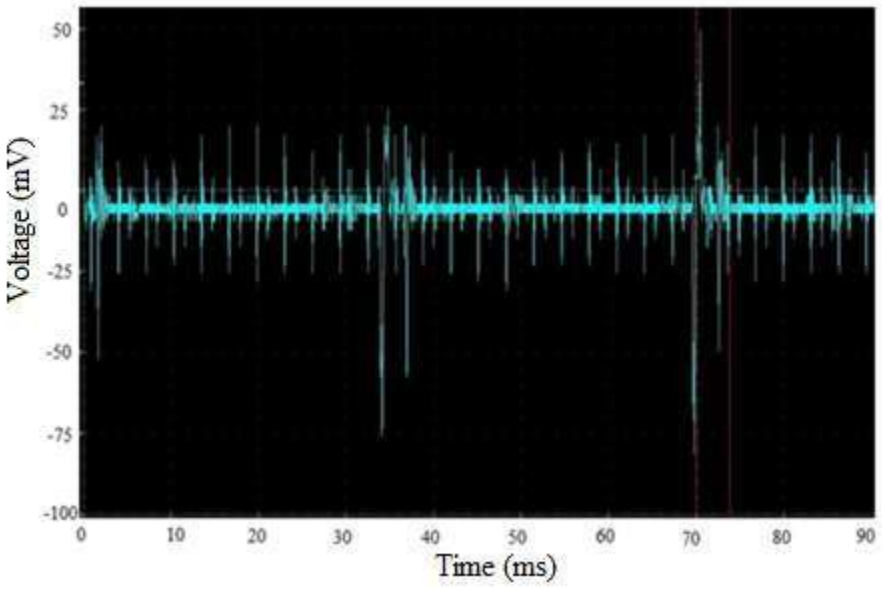


Figure 23: Test and time domain on spinach plant in normal light/ dark and water conditions

Figure 23 show that in normal light/dark and water conditions, the maximum voltage is 25 mV and a minimum of -75 mV. Test and frequency domain analysis on the spinach in normal light/dark and water was done and the results are as shown in Figure 24.

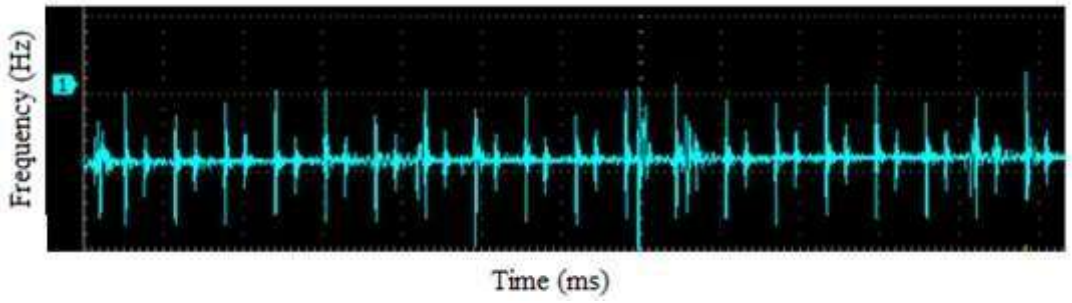


Figure 24. Test and frequency domain on spinach plant in normal light/dark and water condition

The result show that the frequency of the spinach plant in normal light/dark and water condition is 1 Hz. Figure 25 shows the effect of voltage in spinach plant after shaking.

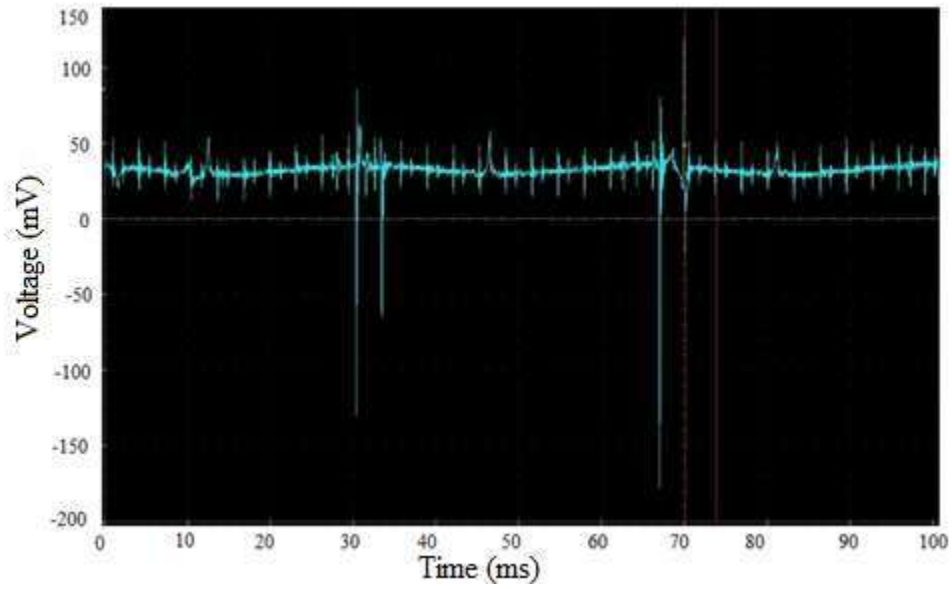


Figure 25. Test and time domain on spinach plant by shaking

After shaking the plant the amplitude of the signal in the test and time graph increases from an average of 25 mV to an average of 50 mV. Figure 26 shows the results of test and frequency domain analysis after shaking the spinach plant.

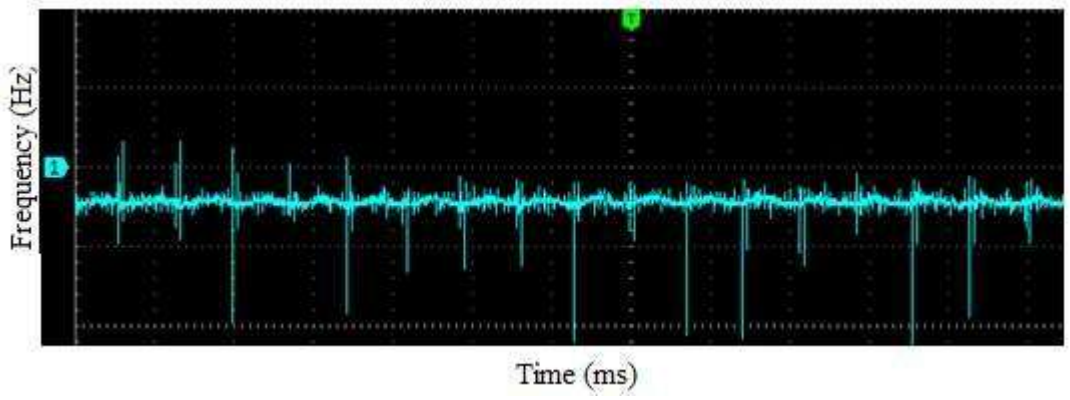


Figure 26: Test and frequency domain on spinach plant by shaking

Test and frequency domain increases, then decreases below 1 Hz and becomes stable. The spinach plant was watered and Figure 27 shows the effect of voltage after watering.

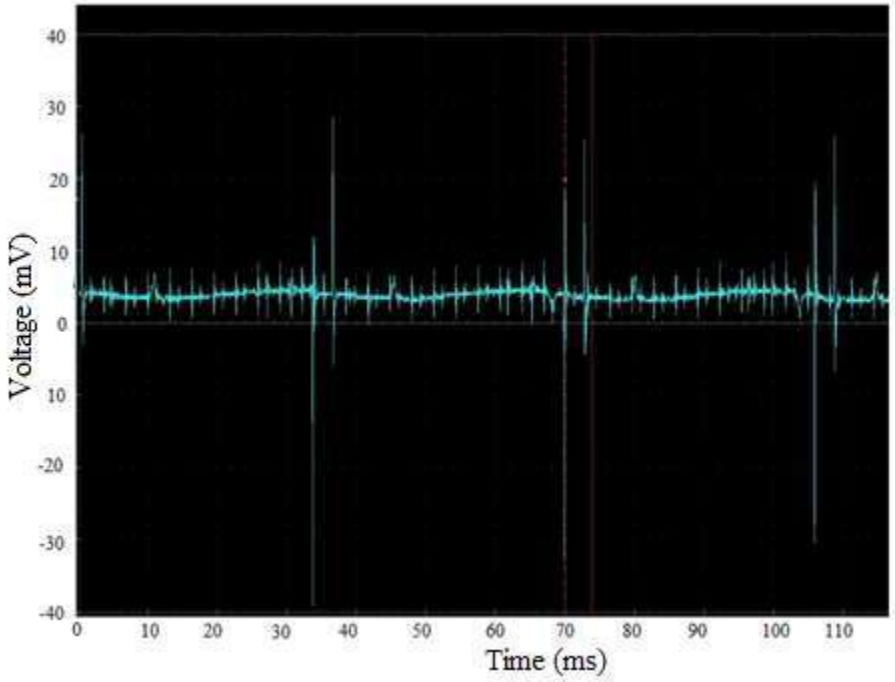


Figure 27: Test and time domain on spinach plant by adding water

Adding water to the spinach decreases the amplitude of the signal from ≈ 25 mV as shown in Figure 23 to ≈ 5 mV in Figure 27. Figure 34 shows decrease in voltage after watering. This demonstrates the existence of measurable electrical potential difference between spinach roots and shoots that can be readily measured and is correlated with soil moisture content. Figure 28 shows the effect of watering on frequency

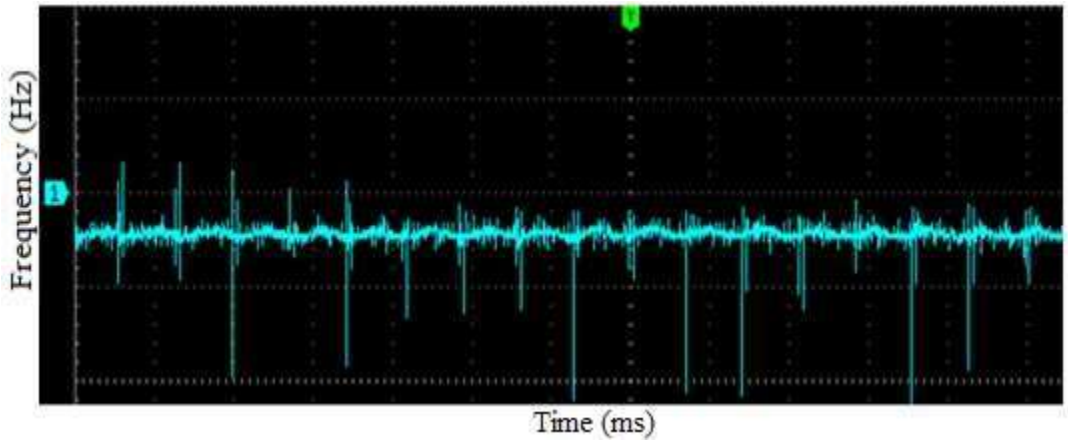


Figure 28: Test and frequency domain on spinach plant by adding water

The graphs show that spinach plant signal is time-varying and unstable and has different frequency components at various times. The frequency varies from 0.5 Hz to a maximum of 1.4 Hz and a minimum 2 Hz.

7. Discussion

Although the op-amp was able to supply +15 V with the input voltage of -5 V, it was unable to supply -15 V with an input voltage of +15 V. This is because the negative rail of the op the op-amp was connected to the ground; which means that the lowest voltage this op-amp can supply is 0 V. The behavior of the output waveform, which suddenly maintains a constant voltage as result of undesired limitations as shown by waveform in figure 11 is known as "clipping". This is solved by powering the negative rail. The aim of frequency analysis was to create such a type of frequency response that will make the op-amp less likely to oscillate. This was achieved by the fact that most of the op-amp are internally compensated (Robert Keim, 2019) and by including an external capacitor. In either case oscillation cannot occur with the positive feedback as long as gain is less than unity. The strategy was to force the op-amp to have a gain less than one at frequencies where the phase difference between the input and output approaches zero. LT spice calculates the total noise within a frequency band by first running the simulation over the frequency band of interest. Then, plot the output noise. The total noise of the above circuit was 2.4605 μV. A large feedback resistor in an op-amp can dominate the noise and make it difficult to see the contribution of the op-amp. The resistors' noise can be turned off by adding a 'noiseless' after the value of the resistor in the schematic as shown in figure 19 and 23. This feature is very important because extra noise from resistors does not have to be subtracted from the measurement. The only noise source is the op-amp. In the time frequency analysis, it was found that the spinach electrical signals in the three cases show peak values of 1 Hz as shown in figure 30, 32 and 34. The peak values appear periodically. Electrical signals have the characteristics of low frequency, which closes to zero hertz. Previous studies have shown that plant electrical signals are of low frequency. Plants electrical signal amplitude arithmetic mean increases with the increase of pulse stimulation signal but for a little effect on the natural frequency of the plant, its frequency is mainly distributed in the 0.07813 Hz-

0.1953 Hz (Weng *et al.,* 2014). The spinach electrical signal voltage is in the microscale and of low frequency of 1 Hz. Environmental changes generate bio-electric potentials in plants (Datta and Palit, 2004). Electrical signals are probably the initial response of the plant to an exterior stimulus (Yan *et al.,* 2009). Analysis in time domain treat plants electric waves as a function of time, through which several characterization of plants can be acquired.

One of the time-frequency domain analysis methods, wavelet transform, enables us to observe certain frequency components or to extract useful characteristic signal. It can be said that this method provides a bright prospect for analysis and measurement of plant electrical signals. Gil et al., 2008 reported that day-to-night fluctuations in EP observed in fruit trees appeared to correspond to the time of day and were therefore presumably affected by diurnal changes which agrees with the results obtained in this work. The results obtained in this work is also similar to results reported by Gil, 2011 which demonstrates the existence of measurable electrical potential difference between avocado roots and shoots that can be readily measured and is correlated with soil moisture content. The effect of a single water application on the EP behavior applied on avocado, showed a sharp EP differential almost immediately after watering followed by a decrease in EP in the minutes that followed (Gurovich & Hermosilla, 2009). In blueberry, irrigation resulted in a sharp, almost instantaneously reduction of EP (Fromm & Spanswick, 2007). In lemon, EP fluctuated rapidly, with an almost instantaneous and short lived increment which was followed by an immediate reduction with respect to the EP value that was measured prior to irrigation (Gurovich & Hermosilla, 2009). After watering, the signal changes (drop in values), and this is attributed to the changes in xylematic water potentials (Oyarce and Gurovich, 2010).

8. Conclusion

The kit designed was able to determine minute EP from spinach plant as it improved the sensitivity and noise filtration. The kit was portable and unique from other instrumentation that have been used in literature. Results show that op-amp has two power supply rails

because they need to swing bipolar-output voltages that go either positive or negative in response to the normal range of input signals. Usually the signals in an op-amp are relatively to a ground that is somewhere between the two rails. Without the dual supplies the output signal would clip at the ground potential. It is also shown that plant electrical signal is a kind of low frequency, small and relatively stable signal. Analysis in timefrequency domain is adopted to acquire satisfying results. Because of the uncertainty of resolution in time or frequency domain, it is not likely to obtain high resolution in time domain and frequency at the same time. The characteristics of plant electrical signals are related to physiological reactions to specific biotic and abiotic stimuli. Plant electrical signal measuring can indirectly reflect plant metabolism, plant vitality and its adaptability to environment

References

Bhagyajyoti, J., Sudheer, L. S., Bhaskar, P., & Parvathi, C. (2012). Review on lock-in amplifier. *Int. J. Sci. Eng. Technol. Res*, *1*(5), 40-45.

Brault M, Amiar Z, Penarun AM, Monestier M, Zhang Z, Cornel D, *et al.* (2004). Plasma membrane depolarization induced by abscisic acid in Arabidopsis suspension cells involves reduction of proton pumping in addition to anion channel activation, which are both Ca2+ dependent. Plant Physiol, 135:1-13.

Brenner ED, Stahlberg R, Mancuso S, Vivanco J, Baluska F, Van Volkenburgh E. (2006). Plant neurobiology: an integrated view of plant signalling. Plant Sci 11:413-9.

Brenner, E. D., Stahlberg, R., Mancuso, S., Vivanco, J., Baluška, F. and Van Volkenburgh, E. (2006). Plant neurobiology: an integrated view of plant signaling. Trends in plant science, 11(8), 413-419.

Cai, W., & Qi, Q. (2017). Study on Electrophysiological Signal Monitoring of Plant under Stress Based on Integrated Op-Amps and Patch Electrode. *Journal of Electrical and Computer Engineering*, *2017*.

Datta, P., & Palit, P. (2004). Relationship between environmental factors and diurnal variation of bioelectric potentials of an intact jute plant. *Current Science*; 87:680-3.

Dong, J., Cheng, Z., & Li, F. (2013). PAHs emission from the pyrolysis of Western Chinese coal. Journal of Analytical and Applied Pyrolysis, 104, 502-507.

Fisahn, J., Herde, O., Willmitzer, L., & Peña-Cortés, H. (2004). Analysis of the transient increase in cytosolic Ca2+ during the action potential of higher plants with high temporal resolution: requirement of Ca2+ transients for induction of jasmonic acid biosynthesis and PINII gene expression. *Plant and Cell Physiology*, *45*(4), 456459.

Fromm, J. and Fei H. (1998). Electrical signalling and gas exchange in maize plants of drying soil. *Plant Science*; 132:203-13.

Fromm, J. and Spanswick, R. (1993). Characteristics of action potentials in willow (Salix viminalis L.). Journalof Experimental Botany, 44(7), 1119-1125.

Fromm, J., & Lautner, S. (2007). Electrical signals and their physiological significance in plants. *Plant, cell & environment*, *30*(3), 249-257.

Gil Montenegro, P. M., Gurovich, L. A., & Iturriaga Agüera, R. (2011). Electrical signal measurements in avocado trees: A potential tool for monitoring physiological responses to soil water content?.

Gil, P. M., Gurovich, L., & Schaffer, B. (2008). The electrical response of fruit trees to soil water availability and diurnal light-dark cycles. *Plant Signaling & Behavior*, *3*(11), 1026-1029.

Gil, P.M., Gurovich, L.A., Schaffer, B., Alcayaga, J. and Iturriaga, R. (2009). November). Electrical signal measurements in avocado trees: a potential tool for monitoring physiological responses to soil water content. In VI International Symposium on Irrigation of Horticultural Crops 889 (pp. 371-378).

Grams, T. E., Koziolek, C., Lautner, S., Matyssek, R., & Fromm, J. (2007). Distinct roles of electric and hydraulic signals on the reaction of leaf gas exchange upon reirrigation in Zea mays L. *Plant, Cell & Environment*, *30*(1), 79-84.

Gurovich, L. A., & Hermosilla, P. (2009). Electric signalling in fruit trees in response to water applications and light–darkness conditions. *Journal of plant physiology*, *166*(3), 290-300.

Isayenkov, S., Isner, J. C., & Maathuis, F. J. (2010). Vacuolar ion channels: roles in plant nutrition and signalling. *FEBS letters*, *584*(10), 1982-1988.

Ives, J. R., & Phelan, S. E. (2010). *U.S. Patent No. 7,643,861*. Washington, DC: U.S. Patent and Trademark Office.

Jingxia, L., & Weimin, D. (2011, October). Study and evaluation of plant electrical signal processing method. In *2011 4th International Congress on Image and Signal Processing* (Vol. 5, pp. 2788-2791). IEEE.

Keim R. (2019). Negative Feedback, Part 1: General Structure and Essential Concepts. Available online. https://www.allaboutcircuits.com/technical-articles/negativefeedback-part-1-general-structure-and-essential-concepts/

Lautner, S., Grams, T. E. E., Matyssek, R., & Fromm, J. (2005). Characteristics of electrical signals in poplar and responses in photosynthesis. *Plant Physiology*, *138*(4), 2200-2209.

Lito, M. G., & Camões, M. F. (2009). Meeting the requirements of the silver/silver chloride reference electrode. *Journal of solution chemistry*, *38*(11), 1471.

Miah, M. A., Nakagawa, Y., Tanimoto, R., Shinjo, R., Kondo, M., & Suzuki, H. (2019). Mass-producible disposable needle-type ion-selective electrodes for plant research. *RSC advances*, *9*(52), 30309-30316.

Moore, K. B., Kimball, T., & Steadman, B. R. U. C. E. (1990). Silver-silver chloride plunge electrode needles and chloriding monitor (bioelectric signal recording application). *IEEE transactions on biomedical engineering*, *37*(5), 532-535.

Oyarce, P. and Gurovich, L. (2011). Evidence for the transmission of information through electric potentials in injured avocado trees. Journal of Plant Physiology. 168(2), 103-108.

Oyarce, P., & Gurovich, L. (2010). Responses to Light and water availability conditions. *Plant Signaling and Behavior*; 5: 34-41.

Oyarce, P., & Gurovich, L. (2010). Responses to Light and water availability conditions. *Plant Signaling and Behavior*; 5: 34-41.

Pyatygin, S. S., Opritov, V. A., & Vodeneev, V. A. (2008). Signaling role of action potential in higher plants. *Russian Journal of Plant Physiology*, *55*(2), 285-291.

Ren, Z., Sun, C., Zhang, J., Ma, L., & Zhao, K. (2019, April). Study on Zero Drift of Charge Amplifier Based on MOSFET 3N165 and OPA LF356N. In *Journal of Physics: Conference Series* (Vol. 1187, No. 2, p. 022044). IOP Publishing.

Rhodes, J., Thain, J., & Wildon, D. (1996). The pathway for systemic electrical signal conduction in the wounded tomato plant. *Plantar*; 200:50-7.

Samhita, V. S. L., Prathyusha, K. L., & Kondaveeti, H. K. (2021, March). A Review on Plant Signal Processing. In *2021 7th International Conference on Advanced Computing and Communication Systems (ICACCS)* (Vol. 1, pp. 124-128). IEEE.

Sanders, D.; Pelloux, J.; Brownlee, C. & Harper, J. F. (2002). Calcium at the Crossroads of

Schaller, A., & Oecking, C. (1999). Modulation of plasma membrane H+-ATPase activity differentially activates wound and pathogen defence responses in tomato plants. *Plant Cell;* 11:263-72.

Sengupta, S. K., Farnham, J. M., & Whitten, J. E. (2005). A simple low-cost lock-in amplifier for the laboratory. *Journal of chemical education*, *82*(9), 1399.

Stolarz, M., & Trębacz, K. (2021). Spontaneous rapid leaf movements and action potentials in Mimosa pudica L. *Physiologia Plantarum*, *173*(4), 1882-1888.

Volkov, A. G., Lang, R. D., & Volkova-Gugeshashvili, M. I. (2007). Electrical signaling in Aloe vera induced by localized thermal stress. *Bioelectrochemistry*, *71*(2), 192197.

Wang, Z. Y., Leng, Q., Huang, L., Zhao, L. L., Xu, Z. L., Hou, R. F., & Wang, C. (2009). Monitoring system for electrical signals in plants in the greenhouse and its applications. *biosystems engineering*, *103*(1), 1-11.

Weng, H. Y., Ye, D. P., Zheng, J. G., Li, H. Y., Liang, X., & Chen, S. H. (2014). Research on characteristics of plant electrical signal under high voltage pulse stimulation. In *Applied Mechanics and Materials* (Vol. 513, pp. 3122-3125). Trans Tech Publications Ltd.

Xu, D., Fang, J., Zhang, M., Wang, H., Zhang, T., Hang, T., ... & Hu, N. (2021). Synchronized intracellular and extracellular recording of action potentials by threedimensional nanoroded electroporation. *Biosensors and Bioelectronics*, *192*, 113501.

Yan, X.;Wang, Z.; Huang, L.;Wang, C.; Hou, R.; Xu, Z.; Qiao, X. (2009). Research progress on electrical signals in higher plants. Prog. Nat. Sci 19, 531–541.

Zebelo, S. A., & Maffei, M. E. (2015). Role of early signalling events in plant–insect interactions. *Journal of Experimental Botany*, *66*(2), 435-448.

Zhao, D. J., Wang, Z. Y., Huang, L., Jia, Y. P., & Leng, J. Q. (2014). Spatio-temporal mapping of variation potentials in leaves of Helianthus annuus L. seedlings in situ using multi-electrode array. *Scientific reports*, *4*(1), 1-7.

Zhao, D. J., Wang, Z. Y., Li, J., Wen, X., Liu, A., Huang, L. & Wang, C. (2013). Recording extracellular signals in plants: A modeling and experimental study. *Mathematical and Computer Modelling*, *58*(3-4), 556-563.

Zimmermann, S., Nürnberger, T., Frachisse, J. M., Wirtz, W., Guern, J., Hedrich, R., & Scheel, D. (1997). Receptor-mediated activation of a plant Ca2+-permeable ion channel involved in pathogen defense. *Proceedings of the National Academy of Sciences*, *94*(6), 2751-2755.